RSC Advances

ROYAL SOCIETY OF CHEMISTRY

www.rsc.org/advances

Cite this: DOI: 10.1039/c0xx00000x

www.rsc.org/xxxxxx

ARTICLE TYPE

Improved Electrochemical Performance of Sulphur Cathodes with Acylated Gelatine as a Binder

Hongyuan Shao,[a] Cheng ming Li,[a] Naiqiang Liu,[a] Weikun Wang,[b] Hao Zhang,[b] Xuhui Zhao*[a] and Yaqin Huang*[a]

Received (in XXX, XXX) XthXXXXXXXXX 20XX, Accepted Xth XXXXXXXXX 20XX
DOI: 10.1039/b000000x

Acylated gelatine has been successfully used in the sulphur cathode for Li/S battery. The results indicated that acylated gelatine could effectively constrain the resolution of polysulphide into the electrolyte because of carbonyl groups' strong affinity for polysulphide. Meanwhile it also served as a strong dispersion and adhesion agent for the cathode materials. Cyclic voltammograms and electrochemical impedance spectroscopy experiments showed that the prepared cathodes have less polarization and lower transfer resistance compared to gelatine binder–sulphur cathode. The prepared cathode exhibited a much higher initial and reversible capacity after 100 cycles at rates of 0.1 and 0.5C than that of gelatine binder–sulphur cathode under the same condition. Our findings have shown that acylated gelatine is a promising binder to improve Li-S performance and helpful for its future development.

1 Introduction

Compared to traditional cathode materials, sulphur has a high theoretical special capacity of 1672 mAh/g and energy density of 2600Wh/kg. The high abundance, nontoxicity and low cost of sulphur make Li/S batteries one of the most promising candidates to replace current state-of-art Li–ion batteries [1]. However, after decades of research and development, the commercialization process of Li/S batteries is still lagged at the initial stage due to several problems: (1) the poor electrode rechargeable performance and limited rate capability [2], mainly owning to the insulation of sulphur and the solid reduction products; (2) high capacity fading rate due to the generation of various soluble polysulphide Li_2S_n ($3 \le n \le 6$) intermediates [3], which leads to a shuttle mechanism; (3) a problematic Li/electrolyte interface [4]. These issues result in low active materials utilization, low coulombic efficiency, and short cycle life of the sulphur cathode [5]. To overcome the hurdles in Li/S battery technology, various approaches have been proposed to enhance the actual capacity and the cycle stability of the sulphur cathode [6-11].Among them, an easy and effective way to design novel sulphur cathode is using appropriate binder, which provides the integrity of sulphur and carbon mixture in the cathodes and is also highly important for improving the performance of the Li/S battery.

Some studies have shown that the utilization of high performance binders can lead to a profound effect on the long–term cycling performance, kinetics and structural stability of electrode materials [12-14]. For example, a recent study showed that the electron–rich groups with lone pairs on oxygen, nitrogen and halogen atoms are capable of binding with lithium in polysulphide Li_2S_n ($4 \le n \le 8$) through a coordination–like interaction. In addition, the strongest interaction with polysulphide was observed in the case of binding with carbonyl groups as those found in esters, ketones and amides [15]. It has also been found that sulphur atom prefers to bond with O atom in –COOH groups in both nitrogen–doped and nitrogen–free carbon. Nitrogen doping can enhance the stabilization of sulphur on –COOH group in the carbon[16]. These works inspired us to increase the amount of specific functional groups such as carbonyl groups in the binder to further improve the performance of Li/S battery.

Our previous work has shown that gelatine was a high adhesion agent and a strong dispersion agent for the cathode materials in Li/S batteries [17,18]. As many functional groups such as $–NH_2$ distribute on the main chain of gelatine, it is easy to introduce more carbonyl groups in gelatine. In this article, we used acylated gelatine as a binder to further explore the effect of carbonyl groups on gelatine binder in the improvement of batteries' electrochemical performance, and to inhibite for the dissolution of polysulphide into electrolyte. The results showed that with the increased amounts of carbonyl groups distributed in the acylated gelatine, more polysulphide Li_2S_n ($4 \le n \le 8$) were confined in the prepared cathode (Scheme. 1) and the acylated gelatine–binder sulphur (SAA) cathodes also exhibited a much higher initial and reversible capacity after 100 cycles at rates of

0.1 and 0.5C than that of gelatine–binder sulphur (SGA) cathode under the same condition.

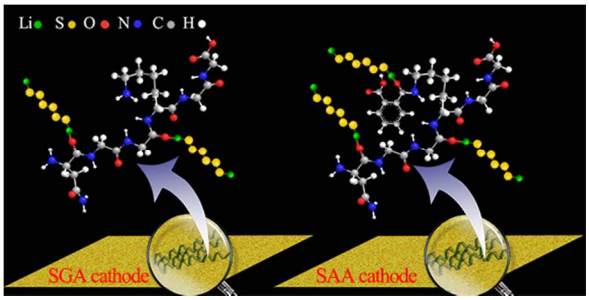

Scheme. 1 Mechanism of mitigating the dissolution of polysulphide into electrolyte using SAA binder.

2 Materials and methods

2.1 Preparation of acylated gelatine.

The gelatine (type B, derived from pig skin) solution (20wt.%) was prepared by dissolving gelatine in deionized water under 60 ℃. Phthalic anhydride (analytical grade, Beijing Yili Fine Chemicals Co., Ltd, China) was then added into the gelatine solution at 40℃with the weight ratio of 10:1 for gelatine and phthalic anhydride. The pH value of the solution was subsequently adjusted to 9.0 using 0.1M sodium hydroxide. After about 30 minutes, 0.05M hydrochloric acid was dropwise added into the solution until reaching the isoelectric point of acylated gelatine. The sample was then filered, washed, and dried.

2.2 Preparation of the cathode

Two types of binder were used to fabricate cathodes. One was acylated gelatine for the SAA cathodes and the other was gelatine for the SGA cathode. The solvent for both binders was water. All sulphur cathode films were prepared by mixing 63wt% sublimed sulphur (99.5%, analytical grade, Beijing, China), 30wt% acetylene black (AB, Jinpu. Corp., China) and 7wt% binder at room temperature. The slurry was then coated onto Al foil. The thickness of all cathode films was about 100 μm and the S loads were about 1.0~1.2mg/cm^2.The fabricated SAA and SGA cathodes were vacuum dried (vacuum degree: 0.1106 pa) at 60℃ for 10 h.

2.3 Li_2S_6-containing electrolyte.

The Li_2S_6-containing electrolyte was prepared by adding small pieces of lithium metal and elemental sulfur (molar ratio of 2:6) in DOL-DME with a final Li_2S_6. The mixture was heated at 80℃ for 1 h to produce a dark yellow solution.

2.4 Experimental measurement.

The Nuclear Magnetic Resonance (^{1}H NMR) spectra of acylated gelatine and gelatine were recorded by Bruker AV–600. All the cathodes were cut into disks with diameter 12 mm to assemble the batteries in an Ar–filled glove box. The anode was lithium foil and the electrolyte was 0.5M lithium bistriuoromethanesulfonylimide (LiTFSI, received from Beijing Chemical Reagent Research Institute) and 0.4 M lithium nitrate in 1,3–dioxolane and 1,2–dime–thoxyethane (volume ratio 1:1, received from Beijing Chemical Reagent Research Institute). The discharge tests were carried out at current densities of 0.1, 0.5, 1, 1.5 and 2C in the voltage range of 1.7–2.8 V, with a LAND–CT2001A instrument under room temperature. The surface morphologies of the cathodes were observed using a scanning electron microscopy (SEM, HITACHIS-4700) operated at 20 kV. Electrochemical impedance spectroscopy (EIS) was measured at open–circuit voltage (OCV) from 100 mHz to 10 kHz at room temperature using the Solartron 1280Z. Cyclic Voltammetry (CV) was also carried out using the same instrument and the scanning rate is 0.1mV/s. UV-visual spectroscopy was measured with TU-1810 to study the soluble species in electrolyte during the discharge process.

Results and discussion

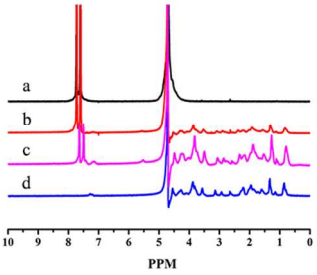

Fig. 1 ^{1}H NMR spectra of phthalic anhydride (a), the mixture of phthalic anhydrid and gelatine (b), acylated gelatine (c)and gelatine (d).

Fig. 1 shows the ^{1}H NMR spectra of acylated gelatine and gelatine. It is clear to see that there are two special peaks for the acylated gelatine at around 7.3 and 7.7 ppm, which are not shown in the gelatine. The special peaks of phthalic anhydride we used in this work are found at 8.0 and 8.42 ppm. The similar pair of peaks in the NMR for acylated gelatine and phthalic anhydride is interpreted as the presence of phthalic anhydride in the acylated gelatine and the chemical shift could be due to the synergistic effect between phthalic anhydride and acylated gelatine, suggesting the successful modification of acylated gelatine by phthalic anhydride.

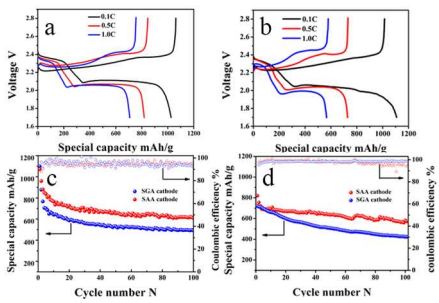

Fig.2 Initial discharge voltage profiles of SAA (a) and SGA (b) cathodes and the cycle performances of the SAA and SGA cathodes at discharge rate of 0.1C (c) and 0.5C (d).

Fig.2a and 2b show the initial discharge voltage profiles of the Li/S batteries with SAA and SGA cathodes at different current rate respectively. When discharged at 0.1C rate, both batteries show an upper plateau at about 2.3 V and a lower plateau at about 2.1 V. With the discharge rate increasing to 0.5 and 1C, these two plateaus of the SAA cathode show a lower voltage drop trend than that of the SGA cathode. It is noteworthy that even at a high discharge rate of 1C, the SAA system maintains two reaction plateaus: the upper one at about 2.3V and the lower one at about 2.1 V. This could be attributed to the weaker polarization of the SAA cathode during discharge process, which has been reported in our previous study [19]. In addition, the upper plateau involves oxidation–reduction reactions between polysulphides (Li_2S_n $4 \leq n \leq 8$) and sulphur (theoretical capacity: 419mAh/g) where the well–known shuttle effect occurs significantly, especially during charging [20]. The longer upper plateau of SAA cathodes indicates lower degree of polysulphides dissolution into the electrolyte and the stronger interaction between polysulphides and carbonyl groups.

The cycling performances of the SAA and SGA cathode at different discharge rates are shown in Fig. 2c and 2d. Compared to the SGA cathode, an improved cycling stability is observed for the SAA cathode at different discharge rates. At a discharge rate of 0.1C, the initial discharge capacity of the SAA cathode is up to 1071 mAh/g (nearly 64% of the theoretical capacity of sulphur), and still has 610 mAh/g after 100 cycles, while the capacity of SGA cathode only fades to 480 mAh/g. As the discharge rate increases to 0.5C, the capacity of SAA cathode after 100 cycles remains 576mAh/g, which is closed to the capacity at 0.1C. However, the capacity of SGA cathodes at 0.5C is only 422 mAh/g and its capacity fading rate was faster than that of SAA cathode. This result may be attributed to the fact that more carbonyl groups distributed in the acylated gelatine, thus stronger interaction between binder and lithium polysulphide presented. The better cycling performance of SAA cathode indicated lower degree of polysulfides dissolution into the electrolyte.

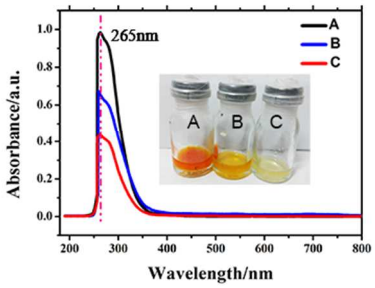

Fig. 3 The UV-visible absorption spectra of Li_2S_6-containing electrolyte (A) with gelatine (B) and acylated gelatine (C), and the inset shows the comparison between A , B and C.

The dark yellow-colored Li_2S_6-containing electrolyte in bottle A was separated equally into three bottles. When we added the gelatine and as-prepared acylated gelatine to bottle B and C, respectively, both of two bottles became light in colour, but the colour of bottle C was obviously lighter than that of bottle B as shown in the inset of Fig. 3, which means strong interaction maybe exists between acylated gelatine and polysulfides. This interesting result attracted us to further investigate the detailed reason by UV-visual spectroscopy. The results show that both of the three samples exhibit a UV absorption band at 265 nm (Fig. 3) which is attributed to Li_2S_6, while the absorption peak of sample C (with acylated gelatine) decreases sharply compared with sample B (with gelatine). From this phenomenon, it is clear to known that much stronger interaction exists between acylated gelatine and polysulphides than that of gelatine, which may be attributed to the abundant number of carbonyl groups existed in acylated gelatine.

.

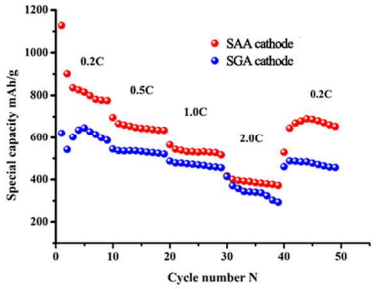

Fig. 4 Rate capability of SAA and SGA cathodes

To check the stability of the binder materials, both SAA and SGA cathodes are cycled at different rate.The data shown in Fig. 4 demonstrate an improved rate capability of SAA and SGA cathodes. The SAA cathode cycling at 0.2, 0.5, 1.0, 2.0C rate show reversible capacities of about 800, 650, 580 and 400mAh/g, respectively. When the rate is switched to 0.2C again, the electrode nearly resumes the original capacity of approximately 750mAh/g. The rate capability of SAA cathode is clearly superior to that of the SGA cathode, indicating that the SAA cathode material is highly robust [21].

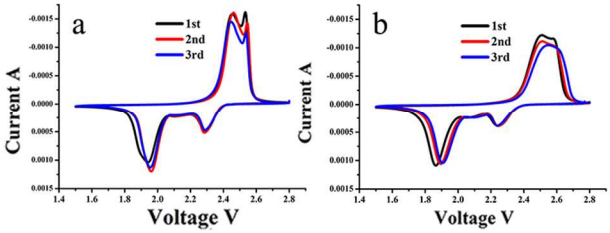

Fig. 5 CV curves of the SAA (a) and SGA (b) cathodes

To investigate the detailed redox reactions of in our Li-S batteries, CV measurements were performed. Fig. 5a and 5b shows the cyclic voltammetry (CV) curves of the SAA and SGA cathodes, respectively. The measurement was conducted at a scan rate of 0.1 mV/s in the voltage range of 1.5 to 2.8 V vs Li/Li^+. During the cathodic scan, two main reduction peaks at around 2.3 and 1.95 V were clearly shown in the curve of SAA cathode. The

peak at around 2.3 V can be assigned to the reduction of elemental S to higher–order Li polysulfides (Li_2S_n, $4 \leq n \leq 8$). The peak at about 1.95 V probably corresponds to the reduction of higher–order Li polysulfides to lower–order Li polysulfides (Li_2S_n, $n < 4$) [22-24]. In the subsequent anodic scan, the big oxidation peak at 2.5V is attributed to the complete conversion of Li_2S and polysulfides into elemental S. [22, 25] Furthermore, from the second cycle, the position and areas of the CV peaks remain nearly unchanged with the increased cycle number, suggesting good reaction reversibility and cycling stability of the SAA electrode [26]. For SAA cathode, smaller voltage gaps, which indicate less polarization, can be identified from the reduction and oxidation peaks [18].This is consistent with the conclusion from measurements in Fig 2.Additionally, the nearly perfect flat anodic base lines indicate that the shuttle effect at SAA cathode has been effectively controlled [27].

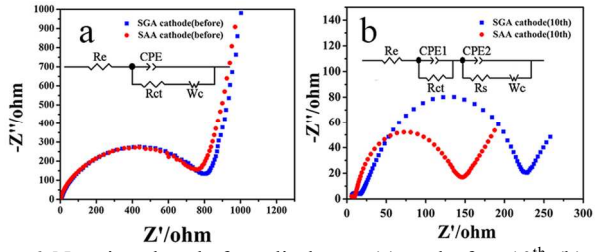

Fig. 6 Nyquist plots before discharge (a) and after 10th (b) of SAA and SGA cathodes

To better understand the improved electrochemical performances with the use of acylated gelatine, the EIS (Fig.6) of SAA cathode and SGA cathode before discharge and after 10 cycles are measured. Before discharging, the impedance spectra are composed of a medium-to-high frequency semicircle and a long inclined line (Warburg impedance) in the low frequency region. The semicircle is attributed to the charge-transfer process at the interface between the electrolyte and sulfur electrode. The Warburg impedance is associated with semi-infinite diffusion of soluble lithium polysulfide in the electrolyte [28, 29]. After 10 cycles, the impedance spectra demonstrate two depressed semicircles followed by a short sloping line. The semicircle in the higher frequency region reflect the interfacial charge transfer process, and the semicircle in the medium frequency range is related to the solid-electrolyte-interface (SEI) film which is caused by the formation of Li_2S (or Li_2S_2) on the carbon matrix in the cathode [28, 29]. The equivalent circuit models for analysing impedance spectra are shown in the inset of Fig. 6a and Fig. 6b, respectively. Re represents the impedance contributed by the resistance of the electrolyte, Rct is the charge transfer resistance at the conductive agent interface, CPE is a constant phase element which is used instead of capacitance and Rs is a deposit diffusion resistance of SEI film. Wc is the Warburg impedance due to the diffusion of the polysulfides within the cathode [28]. As shown in Fig. 6, The Rct of both cathodes before discharge is much higher than that in the 10th cycle. This is due to the high content of sulphur in the cathode possesses very high resistance. After 10 cycles, the resistance of both cells decrease in comparison with that at the beginning, indicating that the irreversible deposition and aggregation of insoluble Li_2S and Li_2S_2 on the surface of SAA and SGA cathodes. The transportation of Li–ions becomes much easier as the cycle number increase, which in turn benefits the high rate capability of the cathode during long cycling [30]. Comparatively, the SAA cathode exhibits lower charge transfer resistance and faster increase rate of conductivity than those of the SGA cathode in the 10th cycle, which may be attribute to the higher sulphur utilization and less shuttle effect. This demonstrates better performance of SAA cathode at long cycle and high charge/discharge rates, as shown in Fig. 2.

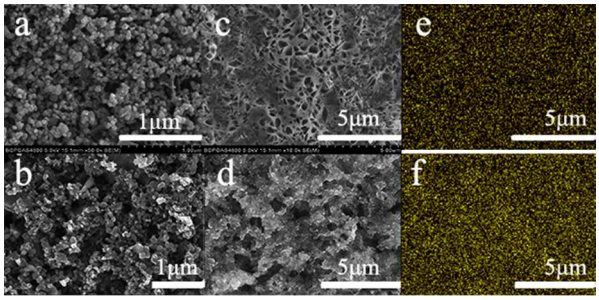

Fig. 7 The SEM images of the sulphur cathodes at charge state during cycling. (a). The pristine SAA cathode. (b). The pristine SGA cathode. (c) The SAA cathode after 100th discharge. (d) The SGA cathode after 100th discharge. Sulphur-distribution mappings of cathodes at 100th discharge obtained from EDS spectra: SAA cathode (e) and SGA cathode (f).

Our previous work for morphology studies has demonstrated that gelatine is a much stronger dispersion and adhesion agent for the cathode materials than that of poly(ethyleneoxide) because gelatine serves as a strong dispersion agent and its aqueous solution has a high viscosity, which makes it suitable as an adhesion agent to bond different types of small particles onto substrates. In this work, the morphology of the SAA cathode and the SGA cathode were also investigated. The SEM images of pristine SAA and SGA cathodes are shown in Fig. 7a and 7b. It is clear to see that sulphur and acetylene black are well distributed in both of the two cathodes. The well dispersion of acetylene black and sulphur can increase the contact area between them and enhance the electrical conductivity. After 100 cycles, the SAA cathode still displays a homogeneous distribution of the cathode materials as shown in Fig. 7c, which is more uniform than that of the SGA cathode shown in Fig. 7d and this could be a reason for SAA cathode's good cyclic durability. The elemental maps of sulphur for the SAA (Fig. 7e) and SGA (Fig. 7f) cathodes after 100th discharge further confirm that the sulphur is homogeneously distributed in both cathodes. Fig. 7 clearly shows that the dispersing and adhesive ability of acylated gelatine binder are also satisfying.

Conclusions

In summary, acylated gelatine has been successfully used as a modified binder in cathode of Li/S battery and has exhibited excellent electrochemical performance in the charge/discharge processes. The initial discharge voltage profiles have reduced the degree of polysulphides dissolution into the electrolyte from SAA cathode. Moreover, an enhanced cycle property of Li/S battery

with an initial capacity of 1071 mAh/g and a high reversible capacity of 610 mAh/g after 100 cycles was achieved with the SAA cathode. The rate capacity tests indicated the SAA cathode material is highly robust and stable. Less polarization and lower shuttle effects were observed in the profile of CV. Lower charge transfer resistances of SAA cathodes before and after 10th discharge further suggested that improved electrochemical stability was achieved through our modification. Therefore, increasing the number of carbonyl groups in the binder can effectively restrain the dissolution of polysulphide and further improve the electrochemical performances in Li/S battery. Our findings are helpful for developing novel binder for Li/S battery in the future and the acylated gelatine binder will be a promising alternative binder for the sulphur cathode.

Acknowledgment

Financial support from the National Science Foundation of China (No. 51272017 and 51432003) and 863 Programs of the National High Technology Research Development Project of China (No. 2012AA052202 and 2011AA11A256) are gratefully appreciated.

Notes and references

[a] *State Key Laboratory of Chemical Resource Engineering, Beijing Laboratory of Biomedical Materials, Beijing University of Chemical University of Chemical Technology, Beijing 100029, People's Republic of China.*

[b] *Research Institute of Chemical Defense, 35 Huayuan North Road, Beijing 100191, PR China.*

* *E-mail:* huangyq@mail.buct.edu.cn*; Fax: +86 10 6443 8266; Tel: +86 10 6443 8266.*

1. M. Cuisinier, P. E. Cabelguen, B. D. Adams, A. Garsuch, M. Balasubramanianc and L. F, *Nazar. Energy Environ. Sci., 2014,7, 2697.*
2. Y. Choi, K. Kim, H. Ahn, J. Ahn, *Journal of Alloys and Compounds, 2008,449,313.*
3. H. Ryu, Z. Guo, H. Ahnc, G. Cho, H. Liu, *Journal of Power Sources, 2009,189, 1179.*
4. P. G. Bruce, S. A. Freunberger, L. J. Hardwick and J.Tarascon, *Nature Materials, 2012,11, 19.*
5. L. Ji, M. Rao, H. Zheng, L. Zhang, Y Li, W. Duan,J. Guo, E. J. Cairns, and Y Zhang, *J. Am. Chem. Soc, 2011, 133, 18522.*
6. H. Wang, Y. Yang, Y. Liang, J. T. Robinson, Y Li, A. Jackson, Y. Cui, and H. Dai, *Nano Lett, 2011, 11, 2644.*
7. N. Jayaprakash, J. Shen, S. S. Moganty, A. Corona, and L. A. Archer, *Angew. Chem. Int. Ed., 2011, 50, 5904.*
8. Z. W. Seh , W. Li , J. J. Cha , G. Zheng , Y. Yang , M. T. McDowell , P. C. Hsu , Y. Cui , *Nat. Commun, 2013 , 4 , 1331 – 1336 .*
9. Z. Liang , G. Zheng , W. Li , Z. W. Seh , H. Yao , K. Yan , D. Kong , Y. Cui , *ACS Nano, 2014 , 8 , 5249 .*
10. J. Zheng , J. Tian , D. Wu , M. Gu , W. Xu , C. Wang , F. Gao , M. H. Engelhard , J. Zhang , J. Liu , J. Xiao , *Nano Lett, 2014 , 14 , 2345.*
11. W. Zhou, Y. Yu, H. Chen , F. J. DiSalvo, H. D. Abruna, *J. Am. Chem. Soc., 2013 , 135 , 16736 .*
12. M. J. Lacey, F. Jeschull, K. Edström, D. Brandell, *Journal of Power Sources, 2014, 264,8.*
13. Y. Wang, Y. Huang,W. Wang, C. Huang, Z. Yu, H. Zhang,J. Sun, A. Wang, K. Yuan, *Electrochimica Acta, 2009,54,4062.*
14. X. Duan, Y. Han, Y. Li and Y. Chen, *RSC Advances, 2014, 4(105),60995.*
15. Z. W. Seh, Q. Zhang, W. Li, G. Zheng, H. Yao and Y. Cui, *Chem. Sci., 2013, 4, 3673.*
16. J. Song , T. Xu , M. L. Gordin , P. Zhu , D. Lv , Y. Jiang , Y. Chen , Y. Duan , and D. Wang, *Adv. Funct Mater, 2014, 24, 1243.*
17. J. Sun, Y. Huang,W. Wang, Z. Yu, A. Wang, K. Yuan, *Electrochimica Acta, 2008,53,7084.*
18. J. Sun, Y. Huang, W. Wang, Z. Yu, A. Wang, K. Yuan, *Electrochemistry Communications. 2008,10,930.*
19. Q. Wang, W. Wang, Y. Huang, F. Wang, H. Zhang, Z. Yu, A. Wang and K. Yuan, *Journal of The Electrochemical Society, 2011,158(6) A775.*
20. Y. Su, Y. Fu, T. Cochell, A. Manthiram. *Nat. Commun, 2013,4,2985.*
21. Z. W. Seh, W. Li, J. J. Cha, G. Zheng, Y. Yang, M. T. McDowell, P. Hsu , Yi Cui, *Nature communications, 2013, 4, 1331.*
22. Zhou, L. C. Yin, D. W. Wang, L Li,. S. Pei, I. R Gentle, F. Li, H. M. Cheng, *ACS Nano, 2013, 7, 5367.*
23. D. Li, F. Han, S. Wang, F. Cheng, Q. Sun, W. C. Li, *ACS applied materials & interfaces, 2013, 5, 2208.*
24. Z, Li. Y, Jiang. L, Yuan. Z, Yi. C, Wu. Y, Liu. P, Strasser, Y. Huang, *ACS Nano2014, DOI: 10.1021/nn503220h.*
25. J. Q. Huang, X. F. Liu, Q. Zhang, C. M. Chen, M. Q. Zhao, S. M. Zhang, W. C. Zhu, W. Z. Qian, F. Wei, *Nano Energy, 2013, 2, 314.*
26. M. J. Lacey, K. Edström, D. Brandell, *Electrochemistry Communications, 2014,46,91.*
27. S. Chen, X. Huang, B. Sun, J. Zhang, H. Liu, G. Wang, *Journal of Materials Chemistry A, 2014, 2(38),16199.*
28. W. G.Wang, X. Wang, L. Y. Tian, Y. L. Wang, S. H. Ye. *Journal of Materials Chemistry A, 2014, 2, 4316–4323.*
29. W. Ahn, K. B. Kim, K. N. Jung, K.-H. Shin, C. S. Jin*, Journal of Power Sources, 2012, 202, 394–399.*
30. X. Gu, Y. Wang, C. Lai, J. Qiu, S. Li, Y. H. W. Martens, N. Mahmood and S. Zhang, *Nano Res, 2014,10,1007.*